Journal of Magnetism and Magnetic Materials 352 (2014) 72–80

Contents lists available at ScienceDirect

Journal of Magnetism and Magnetic Materials

journal homepage: www.elsevier.com/locate/jmmm

First principle study of the electronic structure, Fermi surface, electronic charge density and optical properties of $ThCu_5In$ and $ThCu_5Sn$ single crystals

A.H. Reshak [a,b], Sikander Azam [a,*]

[a] Institute of complex systems, FFPW, CENAKVA-University of South Bohemia in CB, Nove Hrady 37333, Czech Republic
[b] Center of Excellence Geopolymer and Green Technology, School of Material Engineering, University Malaysia Perlis, 01007 Kangar, Perlis, Malaysia

ARTICLE INFO

Article history:
Received 19 June 2013
Received in revised form
4 October 2013
Available online 16 October 2013

Keywords:
FPLAPW calculation
Electronic structure
Charge density
Optical property
DFT

ABSTRACT

The electronic structure, Fermi surface, electronic charge density and optical properties of $ThCu_5In$ and $ThCu_5Sn$ single crystals are studied. The calculations are based on the full potential-linearized augmented plane wave (FPLAPW) method. The exchange and correlation potential is treated by the local density approximation (LDA) and generalized-gradient approximation (GGA), in addition the Engel–Vosko (EV-GGA) formalism was also applied. The DFT calculations show that these compounds have metallic origin. The contribution of different bands was analyzed from total and partial density of states curves. The values of the density of states at Fermi energy ($N(E_F)$) for $ThCu_5In$ ($ThCu_5Sn$) is 1.75 (1.63) states/eV unit cell. The bare electronic specific heat coefficient (γ) is found to be equal to 0.30 and 0.28 mJ/mol-K^2 for $ThCu_5In$ and $ThCu_5Sn$, respectively. The Fermi surface of $ThCu_5In$/$ThCu_5Sn$ is composed of three/four bands crossing along the R–Γ direction. The bonding features are analyzed by using the electronic charge density contour in the (101) crystallographic plane and it shows the covalent character of Cu–Cu and Sn/In–Cu bonds. The optical properties were also calculated and analyzed.

© 2013 Elsevier B.V. All rights reserved.

1. Introduction

Uranium compounds have tempted attention due to many exciting properties which includes the spin fluctuations, Pauli Para magnetism, magnetic ordering, heavy fermions, or superconductivity. In which several properties belongs to the uranium 5f electrons which demonstrate an intermediate quality between the localized 4f electron systems. The job of 5f electrons is significant in actinides and the demand is if they are localized or itinerant or possibly the two configurations coexist giving rise to a new character of the electronic structure, referred to as the duality of the behavior of 5f electrons. It is very effective to evaluate properties of isostructural systems with and without 5f electrons indulgencing the systems with thorium as reference ones. Results of the electronic structure of UCu_5M (M=In, Sn) have freshly been published [1,2]. X-ray phase analyses of $ThCu_5In$ and $ThCu_5Sn$ alloys revealed that they are isostructural and same structure that of UCu_5In(Sn) [3,4]. On the root of a crystallochemical analysis of the compounds cited above, association with simple structural categories in these structures has been recognized. The analysis of their physical properties has verified a number of interesting ending, a summary of which is available in Ref [5]. For example, the powder search of the $U_{1-x}Th_xCu_5In$ solid solutions has powder verified [5] that the exchange of Th for U does not reason an alteration in the crystal structure. A comparable exploration [6] accomplished for the tin compound primed to a similar result, but in this case the Th compound was originated to have a hexagonal unit cell like UCu_5Sn does. In complex compounds containing Cu and elements like In [7] there exists a large number of intrinsic defects which also may give some contribution. The present work reports on structural properties, optical properties and charge density of the $ThCu_5M$ (M=In, Sn) single crystals.

2. Method of calculations

The crystal structure of $ThCu_5In$ and $ThCu_5Sn$ are shown in Fig. 1. The single crystals $ThCu_5In$ and $ThCu_5Sn$ have the orthorhombic structure with space group number 62 (Pnma). The lattice constants for The $ThCu_5Sn$ are a=8.305 Å, b=5.068 Å, c=10.600 Å, and for $ThCu_5Sn$ are a=8.286 Å, b=5.080 Å, c=10.554 Å. The Atomic-positions for $ThCu_5Sn$ and $ThCu_5In$ single crystals are given in Table 1. The investigated, electronic structure and optical properties of the compounds are studied by using WIEN2k code [8]. In this paper the results were obtained by using the highly accurate full

* Corresponding author. Tel./fax: +420 386 361255.
E-mail addresses: sikander.physicst@gmail.com, sikandar_hu@yahoo.com (S. Azam).

0304-8853/$ - see front matter © 2013 Elsevier B.V. All rights reserved.
http://dx.doi.org/10.1016/j.jmmm.2013.10.009

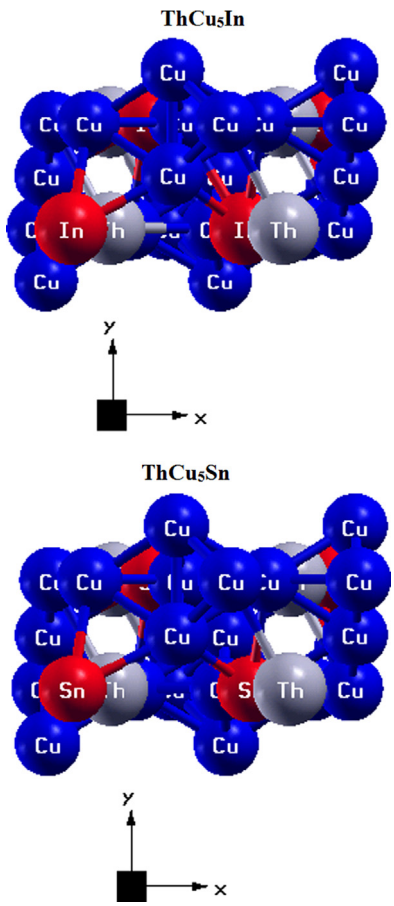

Fig. 1. Unit cell structure for $ThCu_5Sn$/In single crystals.

Table 1
Atomic positions for $ThCu_5Sn$ and $ThCu_5In$ single crystals.

Atoms	X	y	Z
Th(4c)	0.2538 0.2530	0.2500 0.2500	0.5600 0.5579
Cu1(8d)	0.0683 0.0699	0.5011 0.5020	0.3115 0.3116
Cu2(4c)	0.0583 0.0638	0.2500 0.2500	0.1037 0.1029
Cu3(4c)	0.3186 0.3195	0.2500 0.2500	0.2454 0.2460
Cu4(4c)	0.4144 0.4159	0.2500 0.2500	0.0162 0.0174
In(4c)	0.1397	0.2500	0.8604
Sn(4c)	0.1381	0.2500	0.8582

potential linearized augmented plane wave as implemented in theWien2k code, the approach is based on density functional theory (DFT) [9,10] within the LDA, using the scheme of Ceperley–Alderas parameterized by Perdew–Zunger [11], GGA using the scheme of Perdew–Burke–Ernzerhof [12] and EV-GGA as modulated by Engel Vosko [13]. Kohn–Sham wave functions were expanded in terms of spherical harmonic function in side the non-overlapping muffin-tin (MT) spheres and with Fourier series in the interstitial region. The ι-expansions of the wave functions were carried out up to $\iota_{max}=10$ inside the muffin-tin spheres of radius RMT. The Fourier expansion for the charge density was up to $G_{max}=12$. The wave functions in the interstitial regions were expanded in the plane waves for the cut off of $K_{MAX}\times R_{MT}=7$ in order to achieve the convergence for energy Eigen values. The muffin-tin radii of $ThCu_5In$ compound are chosen as: R_{MT} (Th)=2.5 a.u., R_{MT} (Cu)=2.24 a.u and R_{MT} (In)=2.24 a.u and the valve for muffin-tin radii for compound $ThCu_5Sn$ are chosen as R_{MT} (Th)=2.5 a.u., R_{MT} (Cu)=2.35 a.u and R_{MT} (Sn)=2.39 a.u.

For the optical calculations, the dielectric function was calculated in the momentum representation, which requires matrix elements of the momentum p between occupied and unoccupied states. Thus, the components of the imaginary or the absorptive part of the dielectric function, $\varepsilon_2^{ij}(\omega)$, was calculated using the relation given in Ref. [14];

$$\varepsilon_2^{ij}(\omega)=\frac{4\pi^2e^2}{Vm^2\omega^2}\sum_{knn'\sigma}\langle kn\sigma|p_i|kn'\sigma\rangle\langle kn'\sigma|p_j|kn\sigma\rangle \times f_{kn}(1-f_{kn'})\sigma(E_{kn'}-E_{kn}-\hbar\omega) \quad (1)$$

where e is the electron charge and m is the mass, ω is the frequency of the in coming electromagnetic radiation, V is the volume of the unit cell, (px, py, pz)=p is the momentum operator $|kn\sigma\rangle$ the crystal wave function, corresponding to eigen value E_{kn} with crystal momentum k and spin σ. Finally, f_{kn} is the Fermi distribution function ensuring that only transitions from occupied to unoccupied states are counted, and $\sigma(E_{kn'}-E_{kn}-\omega)$ is the condition for total energy conservation. The real part $\varepsilon_1(\omega)$ can be obtained from the imaginary part $\varepsilon_2(\omega)$ using the Kramer's Kronig [15] dispersion relation.

3. Results and discussion

3.1. Band structure and density of states

The electronic band structure which has been calculated for the orthorhombic ThCu5Sn and ThCu5In single crystals are given in Fig. 2. It is clear that the calculated band structure profiles of these compounds using LDA, GGA and EV-GGA are similar with insignificant differences that are attributed to the using different exchange correlations. As noted in the exposed figures that both compounds exhibit a metallic character. As there is no experimental data on the band structure that is available in literatures to be compared with our results, due to successful application of FP-LAPW methods for $ThCu_5In$ and $ThCu_5Sn$ we can discuss the behavior of the energy band structure for this particular material under the current study. Here we set the energy scale in eV, and arbitrarily the energy origin is set to be there at the Fermi level.

To demonstrate the effect of XC potentials, the total density of states for both compounds were calculated using LDA, GGA, and EV-GGA as illustrated in Fig. 3(a) and (b). We have noticed that there are differences in the dispersion of the TDOS upon using LDA, GGA, and EV-GGA. The differences are attributed to the fact that LDA and GGA are based on simple model assumptions which are not sufficiently flexible to reproduce sufficiently the exchange correlation energy and its charge space derivative. The EV-GGA approach is able to reproduce better exchange potential at the expense of less agreement in the exchange energy and yields better band splitting compared to LDA and GGA. Therefore, we have selected EV-GGA for further explanation and demonstrating the partial density of states (PDOS) of these compounds. Fig. 3(c) illustrated the TDOS dispersion of ThCu5In and ThCu5Sn single crystals using EV-GGA. We notice that whole structures of ThCu5Sn are shifted towards lower energies by around 0.5 eV with respect to ThCu5In. The total density of state of both compounds almost similar except the peak that appears at 14.5 eV due to In–d state for ThCu5In single crystals.

In both compounds the peaks between −19.0 eV and −18.0 eV are due to Th–p and Sn–d states and the peaks between −7.0 and −2 eV are due to Cu–d with small contribution of Th–s/d, Cu–s/p,

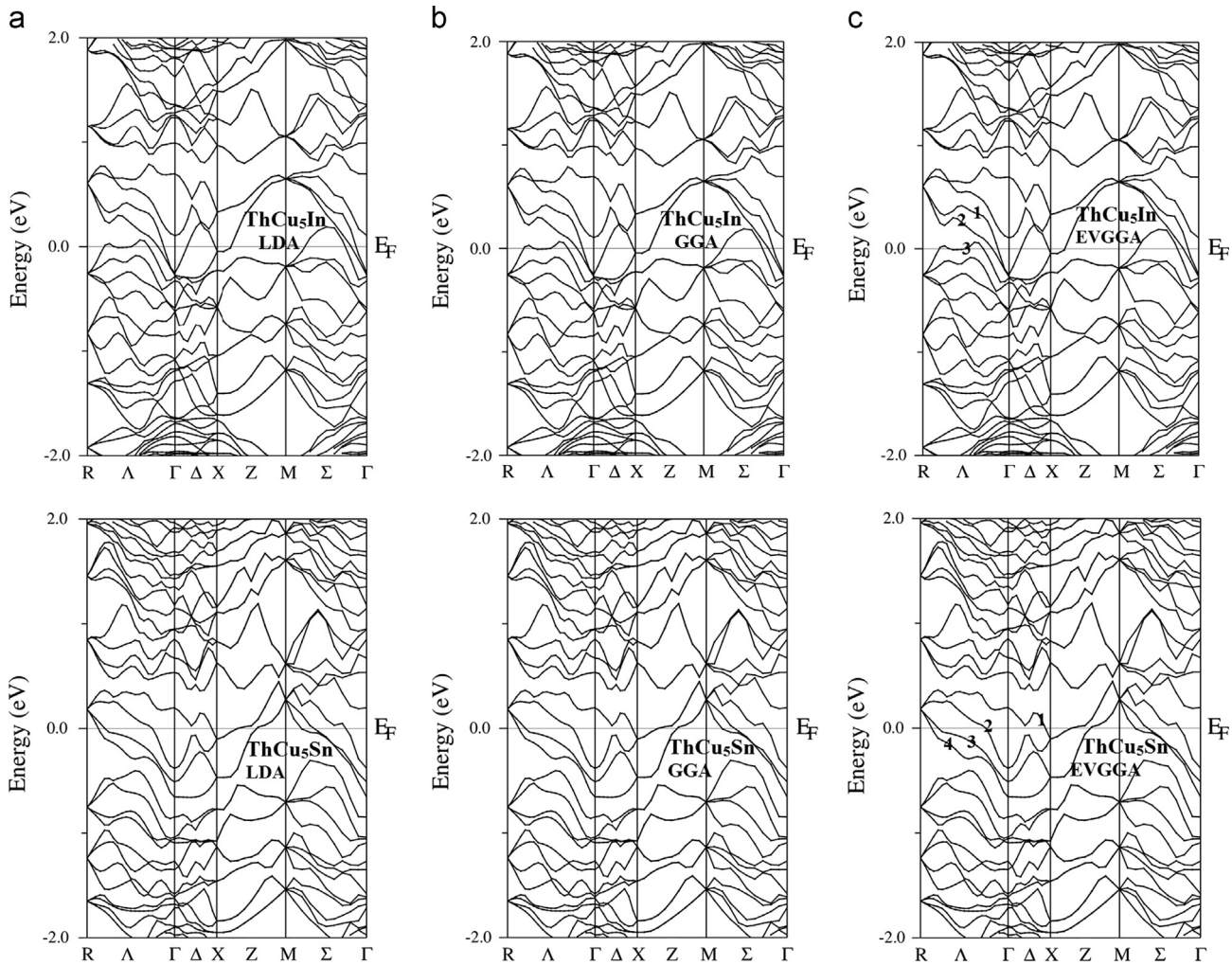

Fig. 2. Calculated band structures for LDA, GGA and EV-GGA for ThCu5Sn and ThCu5In single crystals.

Sn/In–s and Sn–p/d states. The peaks around the Fermi level (E_F) are due to Th–f/d, Sn–d and Cu–s/p states. While the peaks from 2.0 eV and 12.0 eV are due to Th–s/d, Cu–s/p, Sn/In–p and Sn–d states.

As electrons near the Fermi surface are involved in the configuration of the conducting state, it is significant to understand their nature. The total, atomic, and orbital decomposed partial DOS at the Fermi level, $N(E_F)$ has been find.

At E_F the values of DOS at E_F, ($N(E_F)$, for $ThCu_5In$ is 1.75 (states/eV unit cell) and for $ThCu_5Sn$, is 1.63 (states/eV unit cell). The metallic character of the two compounds is clearly seen from the finite DOS at the Fermi level. It is clear from the figures that the $N(E_F)$ is the highest for $ThCu_5In$ as compared to $ThCu_5Sn$. The electronic specific heat coefficient (γ), which is function of $N(E_F)$ can be calculated using the expression

$$\gamma = \frac{1}{3}\pi^2 N(E_F) K_\beta^2 \tag{2}$$

where K_B is the Boltzmann constant. The calculated $N(E_F)$ enables us to obtain the bare electronic specific heat coefficient, which is found to be equal to 0.30 and 0.28 mJ/mol-K^2 for $ThCu_5In$ and $ThCu_5Sn$, respectively.

3.2. Fermi surface

The electrons close to the Fermi level are principally responsible for superconductivity; from the Fermi surface (FS) the electronic structure of any metallic material is understandable. Fermi surfaces can be investigated, for example, using de Haas van Alphen (dHvA) experiments. In this case, the exact determination of the shape of the FS depends on models using easy geometries to define the magnetic field angle dependency of the measured frequencies, but the accurate shape of the FS can of course be much further complex. Therefore we figured the FS of $ThCu_5In$ and $ThCu_5Sn$ single crystals using the FPLAPW method outlined above. The results are shown in Fig. 4.

The calculations for $ThCu_5In$/$ThCu_5Sn$, exposes that there are three/four bands crossing along the R–Γ direction, which is sensitive to changes in the lattice parameters and numerical details of the calculation, as well as band dispersion about the R and Γ point. Changes in the latter band effectually give rise to a modification of the topology of the corresponding Fermi surface sheet for $ThCu_5In$ and $ThCu_5Sn$. Following Fig. 4, these Fermi bands demonstrate a unique complicated "mixed" character: like bands intersects the Fermi level between R and Γ points. These features yield an unusual multi-sheet FS. Indeed, the FS of ThCu5In and $ThCu_5Sn$ single crystals consists of a set of holes and electronic sheets. Empty areas contain holes and shaded areas electrons [18].

In both compounds there are differences in FS topology which are mainly due to changes in inter-atomic distances and bonding angles and as well as to the degree of band filling. For both the compounds, a merged structure is drawn, the changes of color in the Fermi surface occur due to the change in electron velocity. The red color shows fast electron and the violet color shows the slow

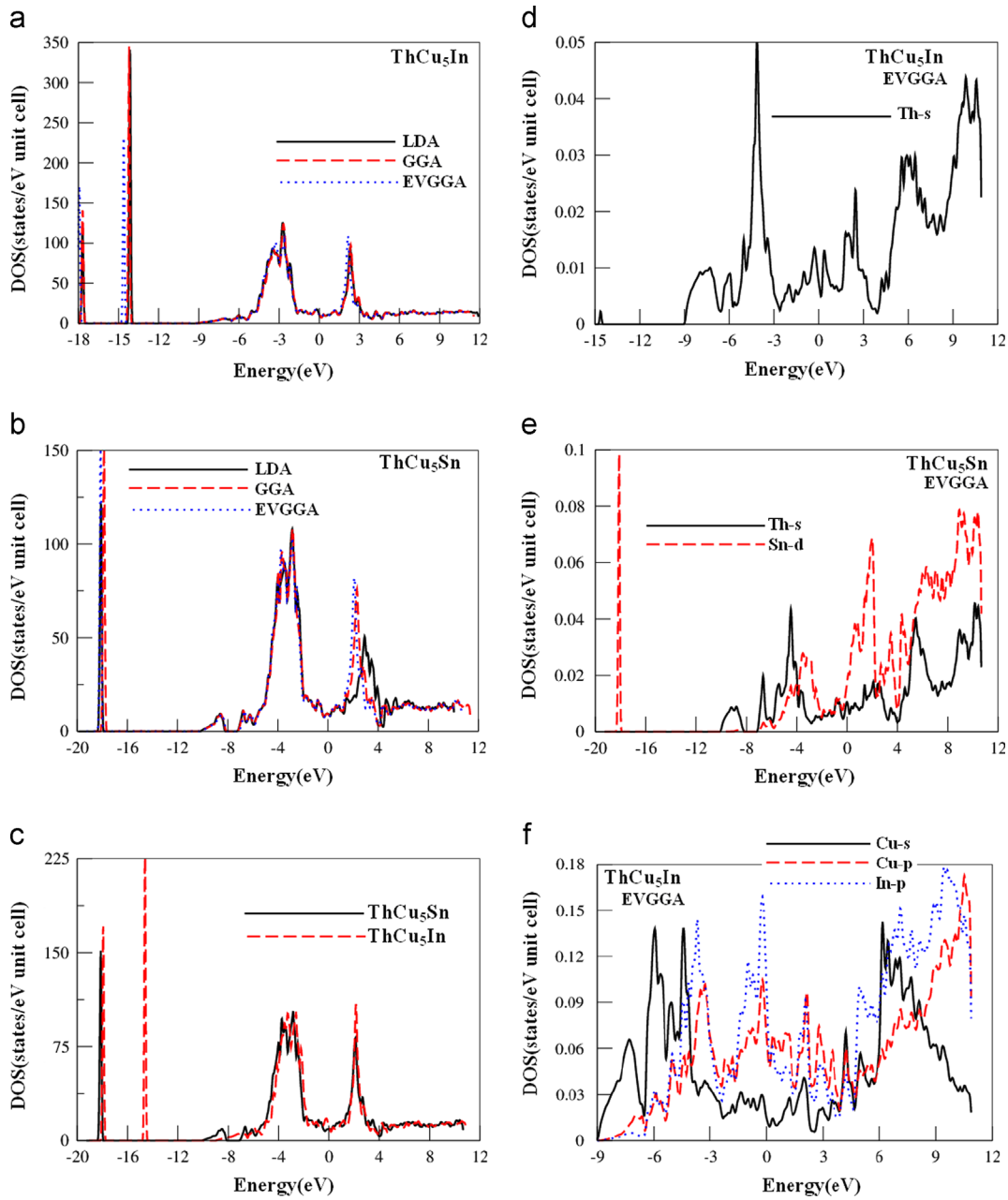

Fig. 3. Calculated total and partial densities of state for ThCu5Sn and ThCu5In single crystals (State/eV unit cell).

electrons and the remaining colors have the intermediate speed of electron [16–19].

3.3. Electron density

Electron density denotes the nature of the bond character. In order to predict the chemical bonding and also the charge transfer in $ThCu_5Sn$ and $ThCu_5In$ single crystals, the charge-density behaviors in 2D are calculated in the (101) plane and displayed in Fig. 5. In order to discuss the electronic charge density we have also calculated the bond lengths in unit lattices of $ThCu_5Sn$ and $ThCu_5In$. The results for bond length are given in Table 2. The result shows that the substitution of the In by Sn leads to redistribution of electron charge density. Replacing an atom by another led to the properties of VSCC (valence shell charge carrier) changes. By investigating the ThCu5Sn and ThCu5In single crystals, the effect of the replacing of In by Sn, the charge density around Sn is greater than In as it is libeled by No. 1 in Fig. 5. The plot is ionic and partial covalent bonding between Cu–Cu and Sn/In–Cu, which acting on the Pauling electro-negativity difference of Cu (1.9) and Sn/In (2.0/1.8) atoms. The calculated electron density shows that charge density lines are spherical in some areas of the plane structure. Which shows sign of ionic bond of the Th atoms, and in some areas of structures Cu and Sn/In atoms shared electron that shows the strong covalent interaction between Cu–Cu and Cu–Sn/In. Since the electro negativity of Sn is greater than that of In, one can naturally expect that charge will be transferred from Th to Sn atoms. That's why in the $ThCu_5Sn$ single crystal the end circle around the Th is not completely circular but there is a little hump. As we replace In by Sn the hump disappears in the $ThCu_5In$ as indicated by No.2 in Fig. 5. The bonding between the Cu–Cu is covalent but in the $ThCu_5In$ the distance between the two nuclei is greater than the $ThCu_5Sn$ because Cu^{+1} and Sn^{+4} repulsive force between the two nuclei is greater comparatively than Cu^{+1} and In^{+3}. Blue color (+1.000) corresponds to the utmost charge gather ion site. So $ThCu_5In$ and $ThCu_5Sn$ single crystals has both ionic and covalent bond. So there is bonding anisotropy in $ThCu_5Sn$ and $ThCu_5In$;

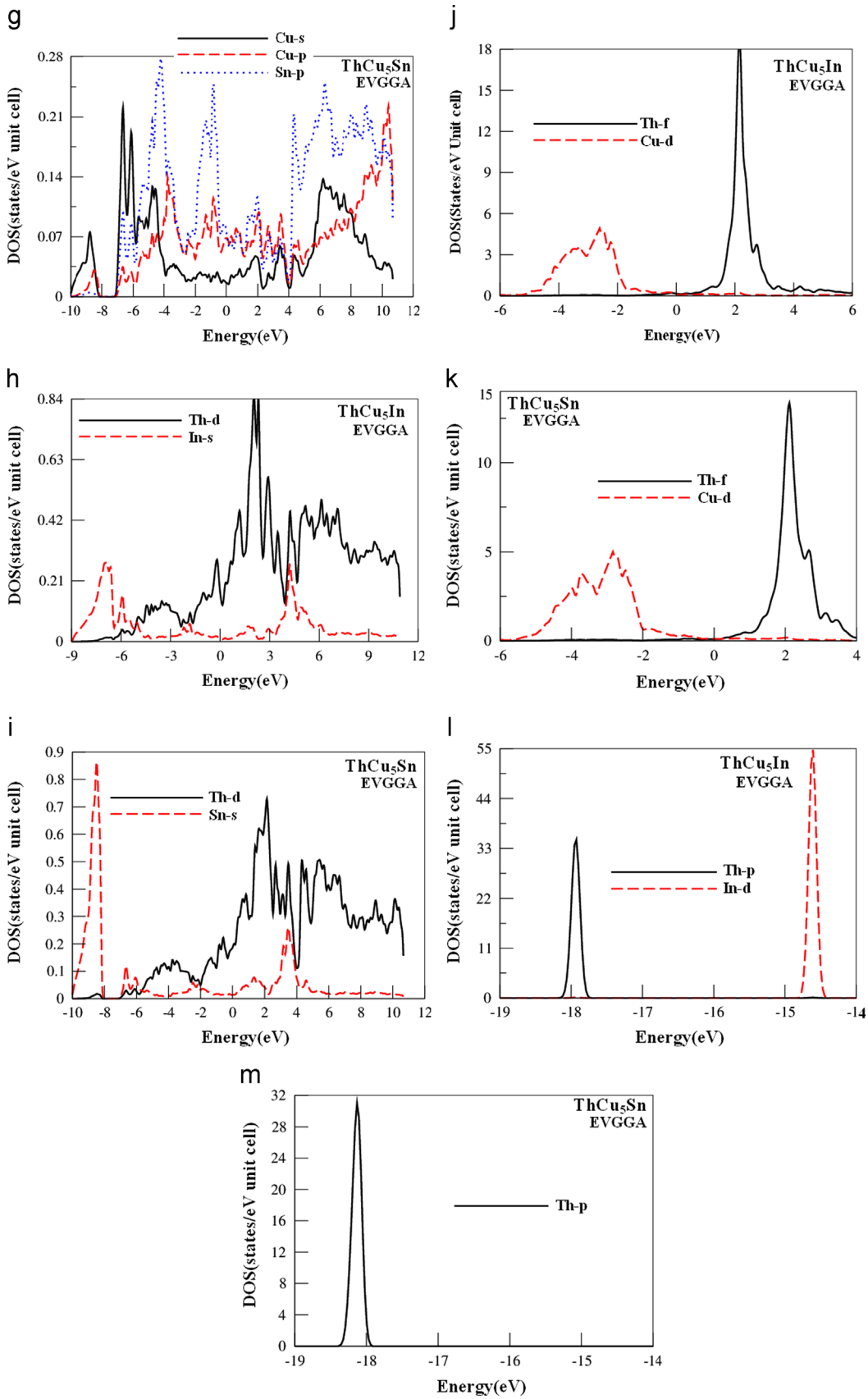

Fig. 3. (*continued*)

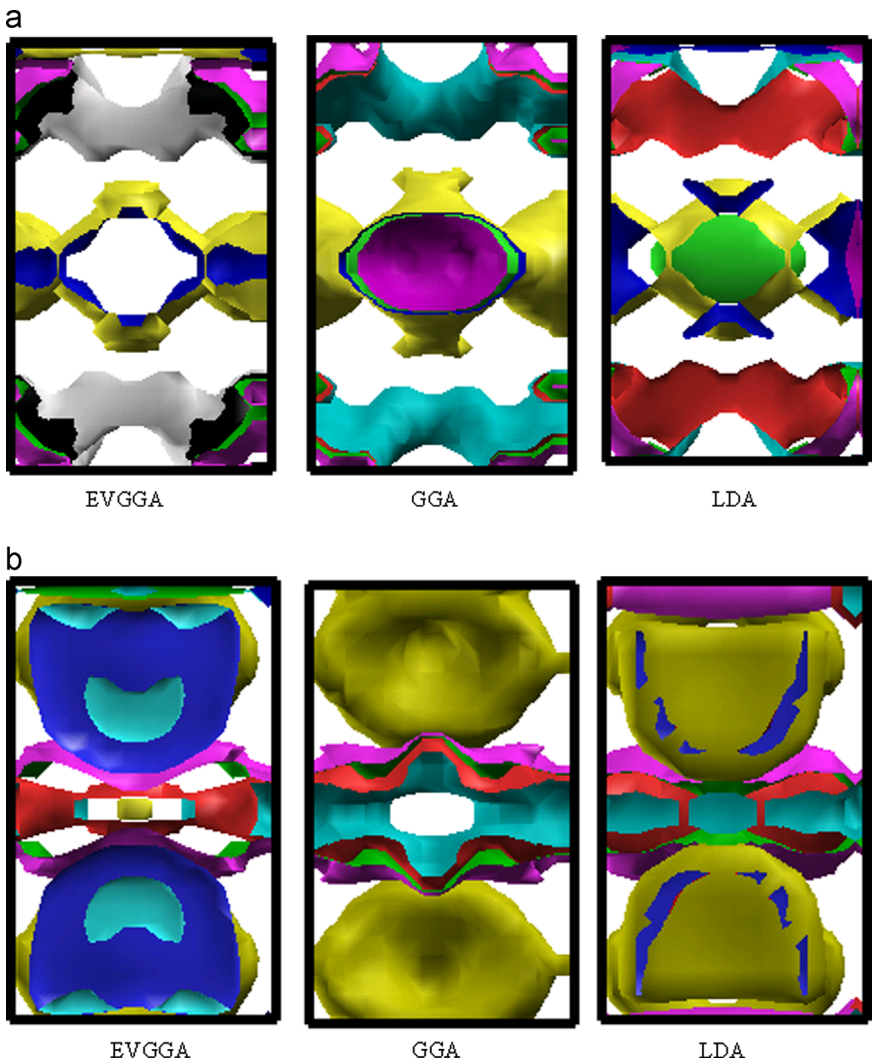

Fig. 4. Fermi surface for $ThCu_5Sn/In$ single crystals.

strongly covalent (Cu–Cu) and (Cu–Sn/In) and strongly ionic (Th) bond in the same structure.

3.4. Optical properties

In solid the optical properties are described by dielectric tensor. The investigated crystals have orthorhombic symmetry, which has only three nonzero components of the second-order dielectric tensor. These are $\varepsilon_2^{xx}(\omega)$, $\varepsilon_2^{yy}(\omega)$ and $\varepsilon_2^{zz}(\omega)$ the imaginary parts of the frequency-dependent dielectric function. These compounds correspond to an electric field perpendicular and parallel to the *c*-axis. As the investigated compounds are metallic so we have to take the intra band transitions (Drude term) into account [15]

$$\varepsilon_2(\omega) = \varepsilon_{2\ \mathrm{int}\ er}(\omega) + \varepsilon_{2\ \mathrm{int}\ ra}(\omega) \tag{3}$$

where

$$\varepsilon_{2\ \mathrm{int}\ ra}(\omega) = \frac{\omega_p^{\tau}}{\omega(1+\omega^2\tau^2)} \tag{4}$$

where ω_p and τ is mean plasma frequency and mean free time respectively among the collisions [20] usually written as:

$$\omega_p^2 = \frac{8\pi}{3}\sum_{kn}\vartheta_{kn}^2\delta(\varepsilon_{kn}) \tag{5}$$

where ε_{kn} is $E_n(k) - E_F$ and ϑ_{kn} is the velocity of electron.

To demonstrate the effect of XC potentials, $\varepsilon_2^{xx}(\omega)$, $\varepsilon_2^{yy}(\omega)$ and$\varepsilon_2^{zz}(\omega)$ were calculated using LDA, GGA, and EV-GGA. Then the average of $\varepsilon_2^{xx}(\omega)$, $\varepsilon_2^{yy}(\omega)$ and$\varepsilon_2^{zz}(\omega)$ components, $\varepsilon_2^{average}(\omega)$, of ThCu5Sn and ThCu5In single crystals were calculated and presented in Fig. 6(a) and (b). Following these figures, one can conclude that EV-GGA shows better result than the other two approximations that is attributed to the fact that EV-GGA shows better band splitting than both of LDA and GGA. So we decided to show the results for EV-GGA only.

Fig. 7(a) and (b), shows the calculated imaginary part $\varepsilon_2^{xx}(\omega)$, $\varepsilon_2^{yy}(\omega)$ and $\varepsilon_2^{zz}(\omega)$ of $ThCu_5Sn$ and $ThCu_5In$ single crystals. As observed from Fig. 7, that the calculated compounds has different optical spectrum as we replace In by Sn the peaks are decreasing. This is accredited to the statistic that there is a contrast in the band structures of these compounds. This causes the changes in the optical transitions in fluctuations the peak heights and positions. We noticed that $\varepsilon_2^{xx}(\omega)$, $\varepsilon_2^{yy}(\omega)$ and $\varepsilon_2^{zz}(\omega)$component shows a considerable anisotropy at low energy, i.e. the components of $ThCu_2Sn$ ($ThCu_2In$) compound show anisotropy between 0.0 eV and 3.5 eV (0.0 eV to 4 eV). Following Fig. 7 one can see that $\varepsilon_2^{xx}(\omega)$ is the dominant component in $ThCu_2Sn$, while $\varepsilon_2^{yy}(\omega)$ is the dominant one in $ThCu_2In$ compound. For $ThCu_5Sn$ ($ThCu_5In$) single crystals, the peak heights of $\varepsilon_2^{xx}(\omega)$, $\varepsilon_2^{yy}(\omega)$ and $\varepsilon_2^{zz}(\omega)$ components are 0.81 eV, 1.04 eV and 0.85 eV (0.45 eV, 0.14 eV and 0.13 eV). When we substitute In by Sn we notice that the peak heights decreased, which shows that the $ThCu_2In$ is more metallic with respect to $ThCu_2Sn$. From the imaginary parts of the dielectric functions $\varepsilon_2^{xx}(\omega)$, $\varepsilon_2^{yy}(\omega)$ and $\varepsilon_2^{zz}(\omega)$ the real parts $\varepsilon_1^{xx}(\omega)$, $\varepsilon_1^{yy}(\omega)$ and

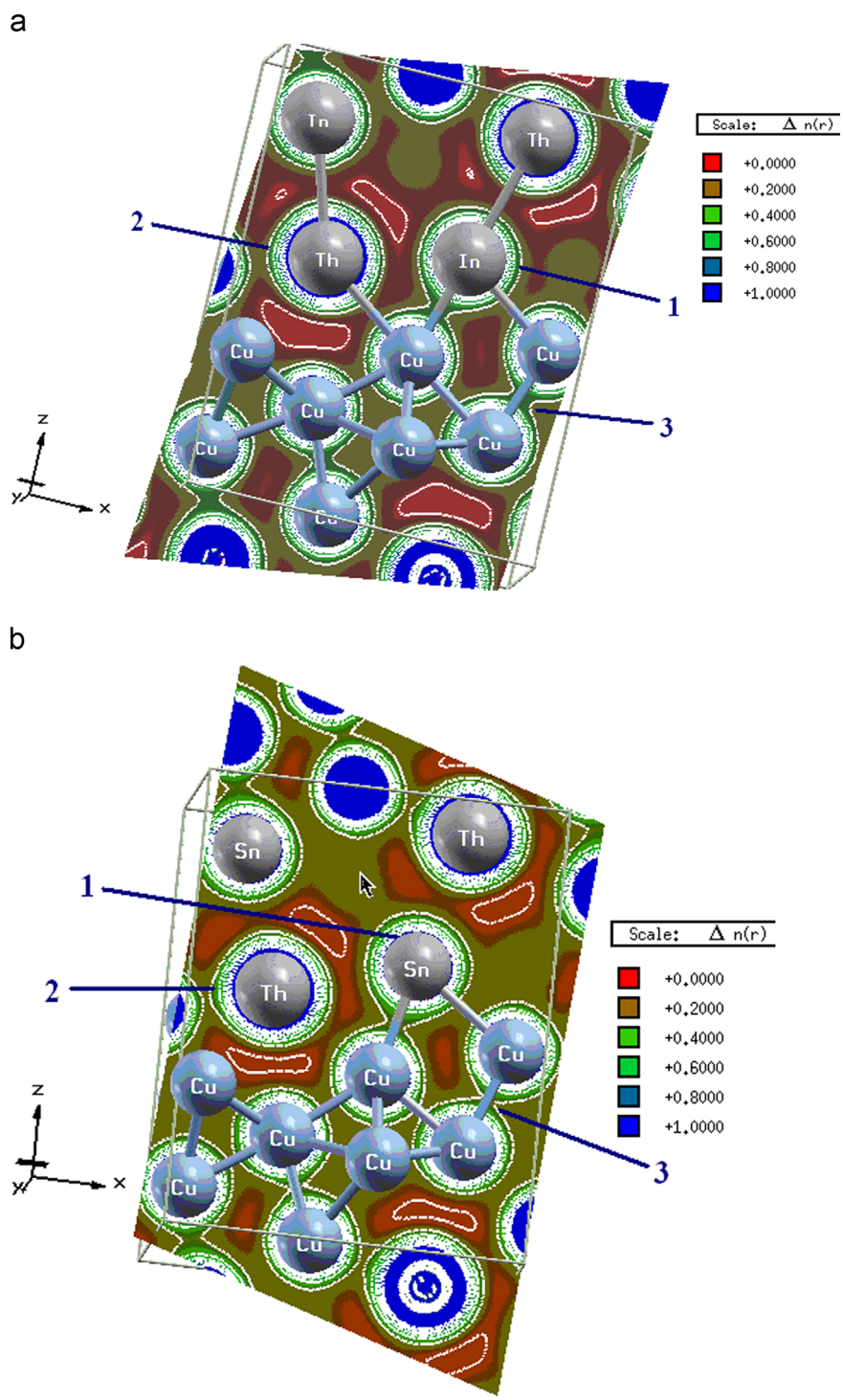

Fig. 5. Calculated charge density for $ThCu_5Sn$ and $ThCu_5In$ single crystals.

Table 2
Bond length.

$ThCu_5Sn$		**$ThCu_5In$**	
Cu_5–Cu_2	2.531 (Å)	Cu_5–Cu_2	2.517 (Å)
Th_1–Sn_6	3.430 (Å)	Th_1–Sn_6	3.466 (Å)
Sn_6–Cu_2	2.760 (Å)	Sn_6–Cu_2	2.799 (Å)
Sn_6–Cu_3	3.046 (Å)	Sn_6–Cu_3	3.989 (Å)
Th_1–Cu_5	2.917 (Å)	Th_1–Cu_5	2.932 (Å)
Th_1–Cu_2	3.236 (Å)	Th_1–Cu_2	3.333(Å)

$\varepsilon_1^{zz}(\omega)$ were calculated by using the Kramers–Kronig relations. The results of $\varepsilon_1^{xx}(\omega)$, $\varepsilon_1^{yy}(\omega)$ and $\varepsilon_1^{zz}(\omega)$ were shown in Fig. 8. It is clear that there is a considerable anisotropy between these three components of the frequency-dependent dielectric function.

4. Conclusion

We performed a detailed investigation on the electronic band structure, density of states, bonding, and linear optical properties of

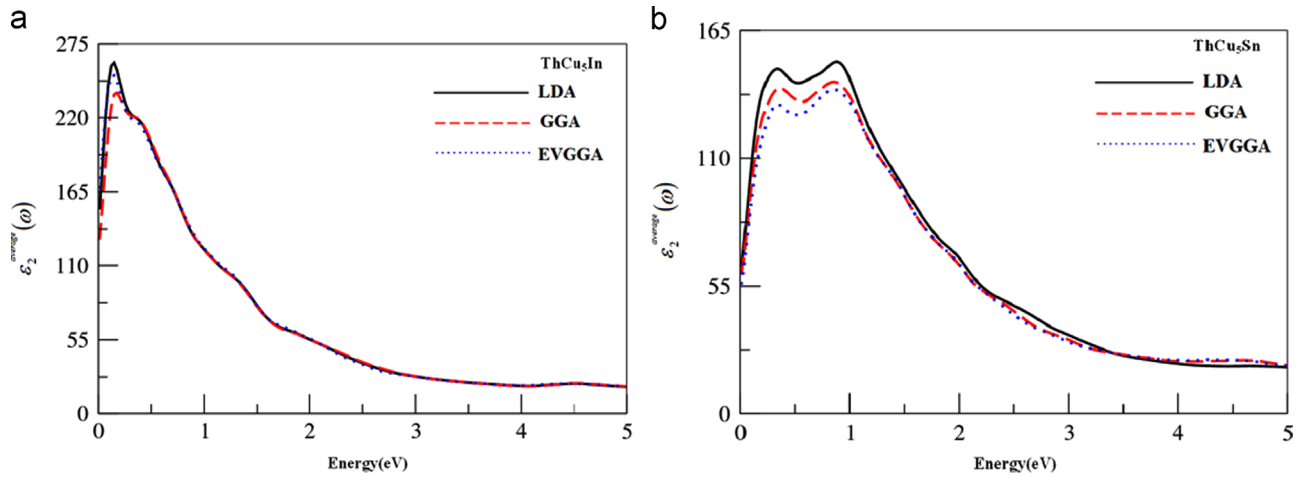

Fig. 6. Calculated average value of imaginary part of dielectric tensor function for $ThCu_5Sn/In$ compounds.

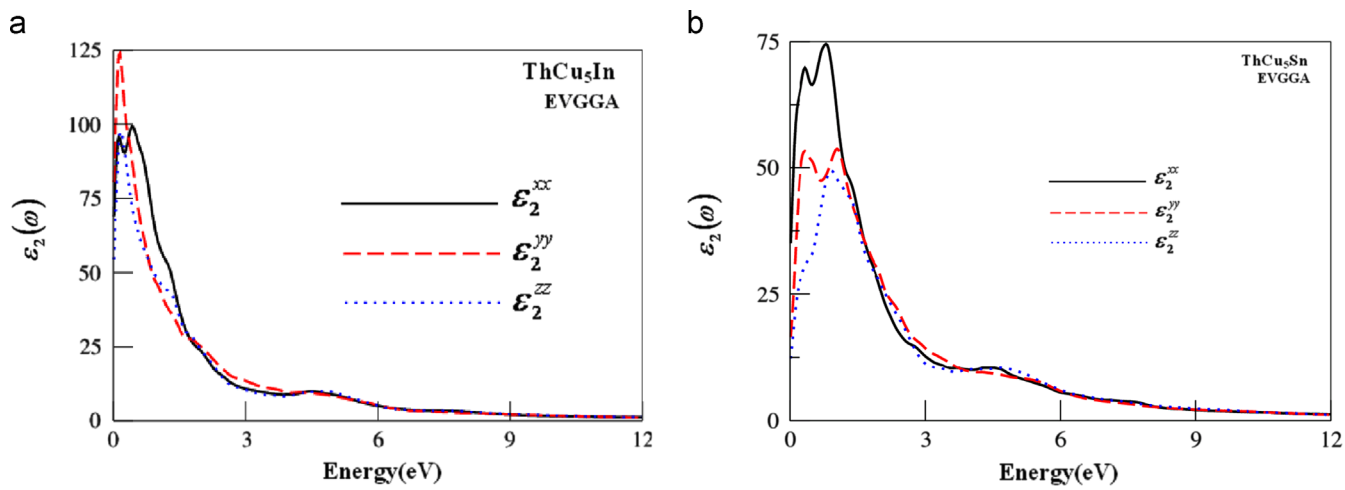

Fig. 7. Calculated imaginary part of dielectric tensor function for $ThCu_5Sn/In$ compounds ($\varepsilon_2(\omega)$).

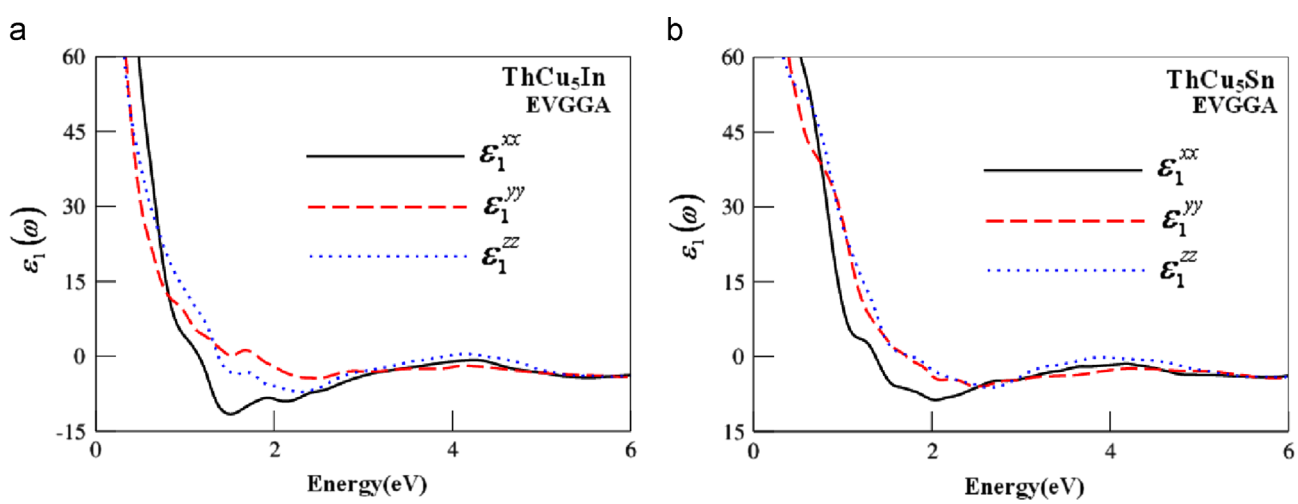

Fig. 8. Calculated real part of dielectric tensor function for $ThCu_5Sn/In$ compound ($\varepsilon_1(\omega)$).

$ThCu_5In$ and $ThCu_5Sn$ single crystals within a framework of DFT based on full potential calculations. The atomic positions of $ThCu_5In$ and $ThCu_5Sn$ are taken from Zaremba et al., and optimized by minimizing the forces acting on the atoms using the FP-LAPW method. The investigated compounds possess metallic nature, the values of DOS at E_F ($N(E_F)$) is 1.75 (1.63) states/eV unit cell, for $ThCu_5In$ and $ThCu_5Sn$, the bare electronic specific heat coefficient (γ) is found to be equal to 0.30 and 0.28 mJ/mol-K^2 for $ThCu_5In$ and $ThCu_5Sn$, respectively. We find that three (four) bands determine the shape the Fermi surface of $ThCu_5In$ ($ThCu_5Sn$). The bonding properties were explained by the investigation of the electronic charge density contour in the (101) crystallographic plane. Following the contour plot there is ionic and

partial covalent bonding between Cu–Cu and Sn/In–Cu atoms. The effect of the replacing of In by Sn, the charge density around Sn is greater than In. The linear optical dispersions namely, the imaginary and real parts of the dielectric function were calculated. With substitute In by Sn we notice that the peak heights decreased, which shows that the $ThCu_2In$ is more metallic with respect to $ThCu_2Sn$. From the imaginary parts of the dielectric functions $\varepsilon_2^{xx}(\omega)$, $\varepsilon_2^{yy}(\omega)$ and $\varepsilon_2^{zz}(\omega)$ the real parts $\varepsilon_1^{xx}(\omega)$, $\varepsilon_1^{yy}(\omega)$ and $\varepsilon_1^{zz}(\omega)$ were calculated by using the Kramers–Kronig relations.

Acknowledgment

This work was supported from the project CENAKVA (No. CZ.1.05/2.1.00/01.0024), the Grant no. 134/2013/Z/104020 of the Grant Agency of the University of South Bohemia. School of Material Engineering, Malaysia University of Perlis, P.O Box 77, d/a Pejabat Pos Besar, 01007 Kangar, Perlis, Malaysia

References

[1] G. Chełkowska, J.A. Morkowski, A. Szajek, R. Troć, J. Phys.: Condens. Matter 14 (2002) 3199.
[2] G. Ghełkowska, J.A. Morkowski, A. Szajek, R. Troć, Phil. Mag. B. 82 (2002) 1893.
[3] V. Zaremba, V. Hlukhyy, J. Stępień-Damm, R. Troć, J. Alloys Compd. 321 (2001) 97.
[4] V. Zaremba, J. Stępień-Damm, R. Troć, D. Kaczorowski, J. Alloys Compd. 280 (1998) 196.
[5] R. Troc, V.H. Tran, D. Kaczorowski, A. Czopnik, Acta Phys. Pol. A 97 (2000) 23–35.
[6] R. Troc, V.H. Tran, B. Andraka, R. Pietri, T. Cichorek, J. Magn. Magn. Mater. 226–230 (2001) 118–120.
[7] G.P. Gorgut, A.O. Fedorchuk, I.V. Kityk, V.P. Sachanyuk, I.D. Olekseyuk, O.V. Parasyuk, Synthesis and structural properties of CuInGeS4, J. Cryst. Growth 324 (2011) 212–216.
[8] P. Blaha, K. Schwarz, J. Luitz WIEN97, A full potential linearized augmented plane wave package for calculating crystal properties, Karlheinz Schwarz, Techn. Universit at Wien, Austria, isbn:3-9501031-0-4, 1999.
[9] P. Hohenberg, W. Kohn, Phys. Rev. 136 (1964) B864.
[10] W. Kohn, L.J. Shom, Phys. Rev. 140 (1965) A1133.
[11] J.P. Perdew, A. Zunger, Phys. Rev. B 23 (1981) 5048.
[12] J.P. Perdew, K. Burke, M. Ernzerhof, Phys. Rev. Lett. 77 (1996) 3865.
[13] E. Engel, S.H. Vosko, Phys. Rev. B 50 (1994) 10498.
[14] A. Delin, P. Ravindran, O. Eriksson, J.M. Wills, Int. J. Quant. Chem. 69 (1998) 349.
[15] F. Wooten, Optical Properties of solids, Academic press, Newyork and London, 1972.
[16] S. Azam, A.H. Reshak., Physica B 431 (2013) 102–108.
[17] A.H. Reshak, S. Azam, J. Magn. Magn. Mater. 345 (2013) 294–303.
[18] A.H. Reshak, S. Azam, J. Magn. Magn. Mater. 342 (2013) 80–86.
[19] A.H. Reshak, S. Azam., Int. J. Electrochem. Sci. 8 (2013).
[20] B. Chakraborrty, WE. Pickett, PB. Allen, Phy. Rev. B 14 (1972) 3227.